Innovative Systems Design and Engineering www.iiste.org
ISSN 2222-1727 (Paper) ISSN 2222-2871 (Online)
Vol 2, No 5, 2011

Comparative Study of Sensorless Control Methods of PMSM Drives

Arafa S. Mohamed, Mohamed S. Zaky, Ashraf S. Zein El Din and Hussain A. Yasin
Electrical Engineering Dept., Faculty of Engineering, Minoufiya University,
Shebin El-Kom (32511), Egypt
E-mail: arafamnsr@yahoo.com

Abstract

Recently, permanent magnet synchronous motors (PMSMs) are increasingly used in high performance variable speed drives of many industrial applications. This is because the PMSM has many features, like high efficiency, compactness, high torque to inertia ratio, rapid dynamic response, simple modeling and control, and maintenance-free operation. In most applications, the presence of such a position sensor presents several disadvantages, such as reduced reliability, susceptibility to noise, additional cost and weight and increased complexity of the drive system. For these reasons, the development of alternative indirect methods for speed and position control becomes an important research topic. Many advantages of sensorless control such as reduced hardware complexity, low cost, reduced size, cable elimination, increased noise immunity, increased reliability and decreased maintenance. The key problem in sensorless vector control of ac drives is the accurate dynamic estimation of the stator flux vector over a wide speed range using only terminal variables (currents and voltages). The difficulty comprises state estimation at very low speeds where the fundamental excitation is low and the observer performance tends to be poor. The reasons are the observer sensitivity to model parameter variations, unmodeled nonlinearities and disturbances, limited accuracy of acquisition signals, drifts, and dc offsets. Poor speed estimation at low speed is attributed to data acquisition errors, voltage distortion due the PWM inverter and stator resistance drop which degrading the performance of sensorless drive. Moreover, the noises of system and measurements are considered other main problems. This paper presents a comprehensive study of the different methods of speed and position estimations for sensorless PMSM drives. A deep insight of the advantages and disadvantages of each method is investigated. Furthermore, the difficulties faced sensorless PMSM drives at low speeds as well as the reasons are highly demonstrated.

Keywords: permanent magnet, synchronous motor, sensorless control, speed estimation, position estimation, parameter adaptation.

1. Introduction

Permanent magnet synchronous motor (PMSM) drives are replacing classic dc and induction motors drives in a variety of industrial applications, such as industrial robots and machine tools [1-3]. Advantages of PMSMs include high efficiency, compactness, high torque to inertia ratio, rapid dynamic response, and simple modeling and control [4]. Because of these advantages, PMSMSs are indeed excellent for use in high-performance servo drives where a fast and accurate torque response is required [5, 6]. Permanent magnet machines can be divided in two categories which are based on the assembly of the permanent magnets. The permanent magnets can be mounted on the surface of the rotor (surface permanent magnet synchronous motor - SPMSM) or inside of the rotor (interior permanent magnet synchronous motor - IPMSM). These two configurations have an influence on the shape of the back electromotive force (back-EMF) and on the inductance variation. In general, there are two main techniques for the instantaneous torque control of high-performance variable speed drives: field oriented control (FOC) and direct torque control (DTC) [7, 8]. They have been invented respectively in the 70's and in the 80's. These control strategies are different on the operation principle but their objectives are the same. They aim both to control effectively the motor torque and flux in order to force the motor to accurately track the command trajectory regardless of the machine and load parameter variation or any extraneous disturbances. The main advantages of DTC are: the absence of coordinate transformations, the absence of a separate voltage modulation block and of a voltage decoupling circuit and a reduced number of controllers. However, on the other hand, this solution requires knowledge of the stator flux, electromagnetic torque, angular speed and position of the rotor [9]. Both control strategies have been successfully implemented in industrial products.

The main drawback of a PMSM is the position sensor. The use of such direct speed/position sensors implies additional electronics, extra wiring, extra space, frequent maintenance and careful mounting which detracts from the inherent robustness and reliability of the drive. For these reasons, the development of alternative indirect methods becomes an important research topic [10, 11]. PMSM drive research has been concentrated on the elimination of the mechanical sensors at the motor shaft (encoder, resolver, Hall-effect sensor, etc.) without deteriorating the dynamic performances of the drive. Many advantages of sensorless ac drives such as reduced hardware complexity, low cost, reduced size, cable elimination, increased noise immunity, increased reliability and decreased maintenance. Speed sensorless motor drives are also preferred in hostile environments, and high speed applications [12, 13].

The main objective of this paper is to present a comparative study of the different speed estimation methods of sensorless PMSM drives with emphasizing of the advantages and disadvantages of each method. Furthermore, the problems of sensorless PMSM drives at low speeds are demonstrated.

2. PMSM Model

The PMSM model can be derived by taken the following assumptions into consideration:

- The induced EMF is sinusoidal
- Eddy currents and hysteresis losses are negligible
- There is no cage on the rotor

The voltage and flux equations for a PMSM in the rotor reference *(d-q)* frame can be expressed as [8]:

$$v_{ds} = R_s i_{ds} + \frac{d\psi_{ds}}{dt} - \omega\psi_{qs} \tag{1}$$

$$v_{qs} = R_s i_{qs} + \frac{d\psi_{qs}}{dt} + \omega\psi_{ds} \tag{2}$$

$$\psi_{ds} = L_d i_{ds} + \psi_r \tag{3}$$

$$\psi_{qs} = L_q i_{qs} \tag{4}$$

The torque equation can be described as:

$$T_e = \frac{3}{2} P[\psi_r i_{qs} - (L_q - L_d) i_{ds} i_{qs}] \tag{5}$$

The equation for the motor dynamic can be expressed as:

$$\frac{d\omega_r}{dt} = \frac{1}{J}(T_e - T_L - F\omega_r) \tag{6}$$

where the angular frequency is related to the rotor speed as follows:

$$\frac{d\theta}{dt} = \omega = P\omega_r \tag{7}$$

where *P* is the number of pole pairs, R_s , is the stator winding resistance, ω is the angular frequency, v_{ds} , v_{qs} , and i_{ds} , i_{qs} are *d-q* components of the stator winding current and voltage, ψ_{ds} and ψ_{qs} are *d-q* components of the stator flux linkage, L_d and L_q are *d* and *q* axis inductances, and ψ_r is the rotor flux linkage. F is the friction coefficient relating to the rotor speed; J is the moment of inertia of the rotor; θ is the electrical angular position of the rotor; and T_e and T_L are the electrical and load torques of the PMSM.

3. Speed Estimation Schemes of Sensorless PMSM Drives

Several speed and position estimation algorithms of PMSM drives have been proposed [14]. These methods can be classified into three main categories. The first category is based on fundamental excitations methods which are divided into two main groups; non-adaptive or adaptive methods. The second category is based on saliency and signal injection methods. The third done is based on artificial intelligence methods. These methods of speed and position estimation can be demonstrated in Figure 1.

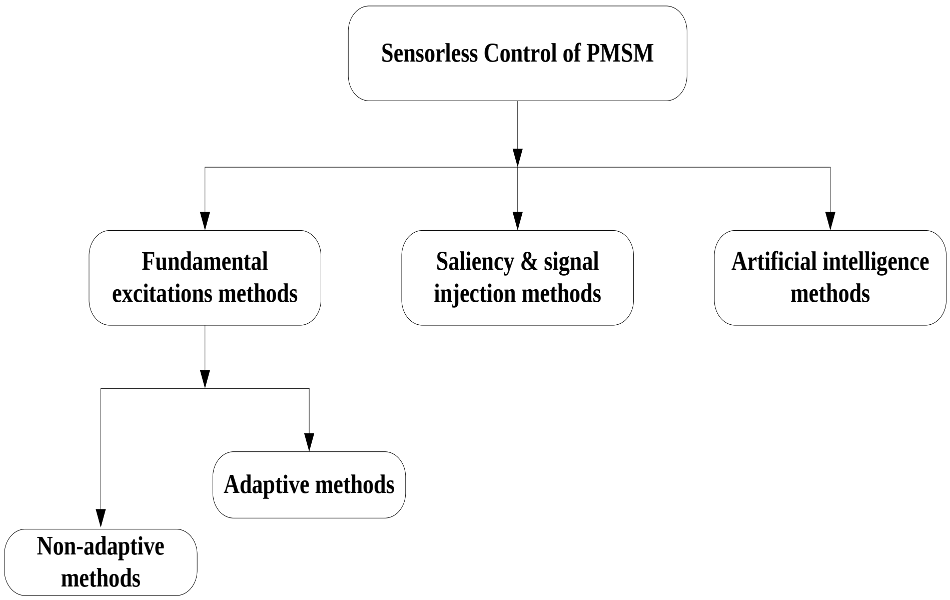

Figure 1. Speed estimation schemes of sensorless PMSM drives.

3.1. Fundamental Excitations Methods

3.1.1 Non-adaptive Methods

Non-adaptive methods use measured currents and voltages as well as fundamental machine equations of the PMSM. The characteristic of this method is easy to be computed, responded quickly and almost no delay. But it required high accurate Motor parameters, more suitable for Motor parameters online identification [2].

A. Estimators using monitored stator voltages, or currents

For estimating the rotor angle θ using measured stator voltages and currents different authors follow different approaches regarding to the used reference frame. This section shows examples for the perspective in three axis and γ-δ coordinates.

[15, 16] propose the approach with the three axis model. Firstly transformation from the *d*-*q* coordinates to the α-β coordinates have to be done. The transformation matrix as follows:

$$T_{dq-\alpha\beta} = \begin{bmatrix} \cos\theta & -\sin\theta \\ \sin\theta & \cos\theta \end{bmatrix} \quad (8)$$

The transformation matrix from the α-β coordinates to the three axis model is illustrated in equation:

$$T_{23} = \begin{bmatrix} 1 & \frac{1}{2} & -\frac{1}{2} \\ 0 & \frac{\sqrt{3}}{2} & \frac{\sqrt{3}}{2} \\ \frac{1}{2} & \frac{1}{2} & \frac{1}{2} \end{bmatrix} \quad (9)$$

The final equation for the rotor position angle can be found as:

$$\theta_r = \tan^{-1}(\frac{A}{B}) \quad (10)$$

Where

$$A = v_{bs} - v_{cs} - R_s(i_{bs} - i_{cs}) - L_d p(i_{bs} - i_{cs}) - \sqrt{3}\omega_r(L_q - L_d)i_{as} \quad (11)$$

$$B = \sqrt{3}(v_{as} - R_s i_{as} - L_d p i_{as}) + \omega_r(L_q - L_d)(i_{bs} - i_{cs}) \quad (12)$$

The position of rotor can thus be obtained in terms of machine voltages and currents in the stator frame provided ω_r in equation can be evaluated in terms of voltages and currents.

[17] Proposes a voltage model and current model based control which works in the γ-δ reference frame with the assumption that $L_d = L_q = L$. The required speed ω_r can be calculated as follows:

$$\omega_r = \frac{\sqrt{C}}{D} \quad (13)$$

$$C = (v_{as} - R_s i_{as} - L_s p i_{as})^2 + \frac{1}{3}(v_{bs} - v_{cs} - R_s(i_{bs} - i_{cs}) - L_s p(i_{bs} - i_{cs}))^2 \quad (14)$$

$$D = \psi_r \quad (15)$$

The initial position of the rotor at t=0 can be determined by substitution ω_r =0 in above equation:

$$\theta_{ro} = \tan^{-1}(\frac{E}{F}) \quad (16)$$

Where:

$$E = \frac{1}{\sqrt{3}}(v_{bs} - v_{cs} - R_s(i_{bs} - i_{cs}) - L_d p(i_{bs} - i_{cs})) \quad (17)$$

$$F = v_{as} - R_s i_{as} - L_d p i_{as} \quad (18)$$

The currents are detected by a current sensor and the voltages are obtained by calculation which using information on PWM pattern, dc voltage and dead time.

The calculation is direct and easy with a very quick dynamic response, and no complicated observer is needed. However, the stator current deviation used in above equations will introduce calculation error due to measurement noise. And any uncertainty of motor parameters will cause trouble to the motor position estimation, which is the biggest problem of this method [18, 19].

B. Flux based position estimators

In this method, the flux linkage is estimated from measured voltages and currents and then the position is predicted by use of polynomial curve fitting [20, 21]. The fundamental idea is to take the voltage equation of the machine,

$$V = Ri + \frac{d\psi}{dt} \tag{19}$$

$$\psi = \int_0^t (V - Ri)dt \tag{20}$$

Where, V is the input voltage, i is the current, R is the resistance, and ψ is the flux linkage, respectively. Based on the initial position, machine parameters, and relationship between the flux linkage and rotor position, the rotor position can be estimated. At the very beginning of the integration the initial flux linkage has to be known precisely to estimate the next step flux linkages. This means that the rotor has to be at a known position at the start [14, 16, and 20]. Last equation (20) written in α-β coordinates depends on the terminal voltage and the stator current. Using the α-β frame the equation for the rotor angle can be written as follows [14, 22]:

$$\theta = \tan^{-1}\left(\frac{\psi_{\alpha s} - Li_{\alpha s}}{\psi_{\beta s} - Li_{\beta s}}\right) \tag{21}$$

where L is the winding inductance.
The actual rotor angle using the d-q frame can be calculated with [14, 22]:

$$\theta = \tan^{-1}\left(\frac{\psi_{ds}}{\psi_{qs}}\right) \tag{22}$$

This method also has an error accumulation problem for integration at low speeds. The method involves lots of computation and is sensitive to the parameter variation. An expensive floating-point processor would be required to handle the complex algorithm [20].

Because of the noise, in the last decade a pure investigation of the rotor position has gained less attention. Solutions with adaptive or observer methods are more common [23, 24].

C. Position estimators based on back-EMF

In PM machines, the movement of magnets relative to the armature winding causes a motional EMF. The EMF is a function of rotor position relative to winding, information about position is contained in the EMF waveform [14].

Paper [25] propagates the determination of the back EMF without the aid of voltage probes which reduces the cost of the system and improves its reliability. Instead of the measured voltages reference voltages are used. The back EMF is not calculated by the integration of the total flux linkage of the stator phase circuits because of the integrator drift problem. The estimation of the rotor position is given by the difference of the arguments of the back EMF in the α-β reference frame and the arguments of the same one in the rotating d-q frame:

$$\theta = \tan^{-1}\left(\frac{e_{\beta s}}{e_{\alpha s}}\right) - \tan^{-1}\left(\frac{\psi_r}{L_q i_{qs}}\right) \tag{23}$$

Previous equation shows, that there is only a quadrature current dependency of the rotor position. Furthermore the back-EMF in subject to the reference voltage in α-β coordinates can be described as following function:

$$f_{(v_{\alpha s}, v_{\beta s})} = \tan^{-1}\left(\frac{v_{\beta s} - R_s i_{\beta s}}{v_{\alpha s} - R_s i_{\alpha s}}\right) \quad (24)$$

The relation between the actual and reference voltages may be written in the form in which the variations $\delta v_{\alpha s}$ and $\delta v_{\beta s}$ are due to the phase difference.

$$\overset{*}{v}_{\alpha s} = v_{\alpha s} + \delta v_{\alpha s} \quad (25)$$

$$\overset{*}{v}_{\beta s} = v_{\beta s} + \delta v_{\beta s} \quad (26)$$

Substituting from previous equations into equation (24), one gets:

$$f_{(\overset{*}{v}_{\alpha s}, \overset{*}{v}_{\beta s})} = f_{(v_{\alpha s}, v_{\beta s})} + \frac{\partial f}{\partial v_{\alpha s}} \delta v_{\alpha s} + \frac{\partial f}{\partial v_{\beta s}} \delta v_{\beta s}$$
$$= \tan^{-1}\left(\frac{\overset{*}{v}_{\beta s} - R_s i_{\beta s}}{\overset{*}{v}_{\alpha s} - R_s i_{\alpha s}}\right) - \frac{V}{E} \omega_r T \quad (27)$$

The second term in this equation is the dependent of the back EMF on the rotor speed. V, E and T are the rms values of the stator voltages, the back EMF and the lag time introduced by the inverter respectively. Thus, we get for the "estimated" position $\overset{*}{\theta}$:

$$\overset{*}{\theta} = \tan^{-1}\left(\frac{\overset{*}{v}_{\beta s} - R_s i_{\beta s}}{\overset{*}{v}_{\alpha s} - R_s i_{\alpha s}}\right) - \frac{V}{E} \omega_r T - \tan^{-1}\left(\frac{\psi_r}{L_q i_{qs}}\right) \quad (28)$$

The proposed algorithm in [25] appears to be robust against parameter variation. Furthermore the electrical drive has a good dynamic performance.

Many control methods suitable for SPMSM cannot be used directly to IPM. In the mathematical model of the IPM, position information is included not only in the flux or EMF term but also in the changing inductance because of its saliency. The model of SPMSM is a special symmetrical case of IPM, which is relatively easy for mathematical procession. In order to apply the method suitable for SPM to a wide class of motors, i.e. the IPM, in [26-28] a novel IPM models are suggested with an extended EMF (EEMF).

By rewriting motor voltage equations into a matrix form:

$$\begin{bmatrix} v_{ds} \\ v_{qs} \end{bmatrix} = \begin{bmatrix} R_s + pL_d & -\omega_r L_q \\ \omega_r L_d & R_s + pL_q \end{bmatrix} \begin{bmatrix} i_{ds} \\ i_{qs} \end{bmatrix} + \begin{bmatrix} 0 \\ \omega_r \psi_r \end{bmatrix} \quad (29)$$

There are two trigonometric functions of *2θ*, which result from changing stator inductance. A reason why *2θ* terms appear can be concluded as that the impedance matrix is asymmetrical. If the impedance matrix is rewritten symmetrically as:

$$\begin{bmatrix} v_{ds} \\ v_{qs} \end{bmatrix} = \begin{bmatrix} R_s + pL_d & -\omega_r L_q \\ \omega_r L_q & R_s + pL_d \end{bmatrix} \begin{bmatrix} i_{ds} \\ i_{qs} \end{bmatrix} + \begin{bmatrix} 0 \\ (L_d - L_q)(\omega_r i_{ds} - p i_{qs}) + \omega_r \psi_r \end{bmatrix} \quad (30)$$

The circuit equation on *α-β* coordinate can be derived as follows, in which there is no *2θ* term.

$$\begin{bmatrix} v_{\alpha s} \\ v_{\beta s} \end{bmatrix} = \begin{bmatrix} R_s + pL_d & \omega_r (L_d - L_q) \\ -\omega_r (L_d - L_q) & R_s + pL_d \end{bmatrix} \begin{bmatrix} i_{\alpha s} \\ i_{\beta s} \end{bmatrix} + \{(L_d - L_q)(\omega_r i_{ds} - p i_{qs}) + \omega_r \psi_r\} \begin{bmatrix} -\sin\theta \\ \cos\theta \end{bmatrix} \quad (31)$$

The second term on the right side of (31) is defined as the extended EMF (EEMF). In this term, besides the traditionally defined EMF generated by permanent magnet, there is a kind of voltage related to saliency of IPMSM. It includes position information from both the EMF and the stator inductance. If the EEMF can be estimated, the position of magnet can be obtained from its phase just like EMF in SPMSMs. Generally the position estimation calculated from the EEMF [14, 18]:

$$e = \begin{bmatrix} e_{\alpha s} \\ e_{\beta s} \end{bmatrix} = \{(L_d - L_q)(\omega_r i_{ds} - p i_{qs}) + \omega_r \psi_r\} \begin{bmatrix} -\sin\theta \\ \cos\theta \end{bmatrix} \quad (32)$$

$$\theta = \tan^{-1}\left(-\frac{e_{\beta s}}{e_{\alpha s}}\right) = \left(\frac{v_{\alpha s} - (R_s + pL_d) i_{\alpha s} - \omega_r (L_d - L_q) i_{\beta s}}{v_{\beta s} - (R_s + pL_d) i_{\beta s} + \omega_r (L_d - L_q) i_{\alpha s}}\right) \quad (33)$$

The problem is that, the EEMF is influenced by stator current i_{ds} and i_{qs}, which vary during motor transient state. This will cause troubles to the speed estimation. In the low speed range, the signal to noise ratio of the EEMF is relatively small and the speed estimation result is still not so good. To overcome this difficulty several authors uses observer and adaptive methods [14].

3.1.2 Adaptive Methods

In this category, various types of observers are used to estimate rotor position. The fundamental idea is that a mathematical model of the machine is utilized and it takes measured inputs of the actual system and produces estimated outputs. The error between the estimated outputs and measured quantities is then fed back into the system model to correct the estimated values adaptation mechanism. The biggest advantage of using observers is that all of the states in the system model can be estimated including states that are hard to obtain by measurements. Also, in the observer based methods, the error accumulation problems in the flux calculation methods do not exist [20], but the weakness is poor speed adjustable at low speed, complicated algorithm and huge calculation [2]. Observers have been implemented in sensorless PM motor drive systems. The adaption mechanism base on the following three methods criteria of super stability theory (Popov), kalman filter, and method of least error square [29]. Methods using the Popov are criteria model reference adaptive system and luenberger observer.

A. Estimator Based on Model Reference Adaptive System

A model reference adaptive system (MRAS) can be represented by an equivalent feedback system as shown in Figure 2.

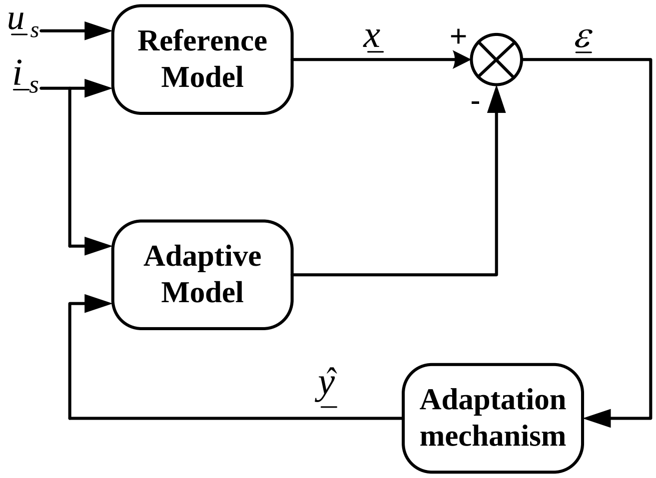

Figure 2. Rotor speed estimation structure using MRAS.

Where ε represents the error between the reference model and the adaptive model. The difference between real and estimated value can be expressed with the dynamic error equation [29]:

$$\frac{d\underline{\varepsilon}}{dt} = \frac{d}{dt}(\underline{x} - \underline{\hat{x}}) = A\underline{x} - \hat{A}\underline{\hat{x}} - K(C\underline{x} - C\underline{\hat{x}}) \qquad (34)$$
$$= (A - KC)\,\underline{\varepsilon} + (A - \hat{A})\,\underline{\hat{x}}$$

Where $\underline{x}$ is the state vector, $\underline{u}$ the system input vector, $\underline{y}$ the output vector, the matrices ***A*** , ***B*** and ***C*** the parameter of the PMSM and the matrix ***K*** a gain coefficient respectively. All elements with ^ are the estimated vectors and matrices.

It should be noted that, speed estimation methods using MRAS can classified into various types according to the state variables. The most commonly used are the rotor flux based MRAS, back-emf based MRAS, and stator current based MRAS. For all mentioned states can be applied one adaption model [29]:

$$\hat{y} = k_p(x_q x_d - \hat{x}_q x_d) + k_i \int_0^T (x_q x_d - \hat{x}_q x_d)\,dt \qquad (35)$$

Stability and speed of the calculation of $\hat{y}$ depends on the proportional and integral part of (35). x_q and x_d represent the states of the PMSM in quadrature and direct coordinates.

As the rotor speed ω is included in current equations, we can choose the current model of the PMSM as the adaptive model, and the motor itself as the reference model. These two models both have the output i_{ds} and i_{qs} , According to the difference between the outputs of the two models, through a certain adaptive mechanism, we can get the estimated value of the rotor speed. Then the position can be obtained by integrating the speed [30].

The equations (1) to (4) can be written as below form:

$$L_d \frac{di_{ds}}{dt} = -R_s i_{ds} + \omega L_q i_{qs} + v_{ds} \qquad (36)$$

$$L_q \frac{di_{qs}}{dt} = -R_s i_{qs} - \omega L_d i_{ds} - \omega \psi_r + v_{qs} \qquad (37)$$

The *d*-*q* axis currents i_{ds} , i_{qs} are the state variables of the current model of the PMSM, which is described by (36) and (37).

By rewriting equations (36) and (37) into a matrix form as below:

$$\frac{d}{dt}\begin{bmatrix} i_{ds}+\frac{\psi_r}{L_d} \\ i_{qs} \end{bmatrix} = \begin{bmatrix} -\frac{R_s}{L_d} & \omega\frac{L_q}{L_d} \\ -\omega\frac{L_d}{L_q} & -\frac{R_s}{L_q} \end{bmatrix}\begin{bmatrix} i_{ds}+\frac{\psi_r}{L_d} \\ i_{qs} \end{bmatrix} + \begin{bmatrix} \frac{v_{ds}}{L_d}+\frac{R_s\psi_r}{L_d} \\ \frac{v_{qs}}{L_q} \end{bmatrix} \tag{38}$$

For the convenience of stability analysis, the speed ω has been confined to the system matrix:

$$A = \begin{bmatrix} -\frac{R_s}{L_d} & \omega\frac{L_q}{L_d} \\ -\omega\frac{L_d}{L_q} & -\frac{R_s}{L_q} \end{bmatrix} \tag{39}$$

To be simplified, define:

$$x = \begin{bmatrix} x_1 \\ x_2 \end{bmatrix} = \begin{bmatrix} i_{ds}+\frac{\psi_r}{L_d} \\ i_{qs} \end{bmatrix} \tag{40}$$

$$u = \begin{bmatrix} u_1 \\ u_2 \end{bmatrix} = \begin{bmatrix} \frac{v_{ds}}{L_d}+\frac{R_s\psi_r}{L_d} \\ \frac{v_{qs}}{L_q} \end{bmatrix} \tag{41}$$

Then the reference model can be rewritten as:

$$\frac{d}{dt}x = Ax + u \tag{42}$$

The adaptation mechanism uses the rotor speed as corrective information to obtain the adjustable parameter current error between two models in order to drive the current error to zero, when we can take the estimation value as a correct speed. The process of speed estimation can be described as follows:

$$\frac{d}{dt}\begin{bmatrix} \hat{x}_1 \\ \hat{x}_2 \end{bmatrix} = \begin{bmatrix} -\frac{R_s}{L_d} & \hat{\omega}\frac{L_q}{L_d} \\ -\hat{\omega}\frac{L_d}{L_q} & -\frac{R_s}{L_q} \end{bmatrix}\begin{bmatrix} x_1 \\ x_2 \end{bmatrix} + \begin{bmatrix} \hat{u}_1 \\ \hat{u}_2 \end{bmatrix} \tag{43}$$

Where $\hat{\omega}$ is to be estimated, (43) can be simplified as below:

$$\frac{d}{dt}\hat{x} = \hat{A}\hat{x} + u \qquad (44)$$

The error of the state variables is:

$$e = x - \hat{x} \qquad (45)$$

According to equation (42) and (44), estimation equation can be written as:

$$\frac{d}{dt}e = Ae - Iw \qquad (46)$$

$$v = De \qquad (47)$$

Where $w = (\hat{A} - A)\hat{x}$, choose $D = I$, then

$$v = Ie = e \qquad (48)$$

According to Popov super stability theory, if

(1) $H(s) = D(SI - A)^{-1}$ is a strictly positive matrix,

(2) $\eta(0,t_0) = \int_0^{t_0} v^T w dt, \forall t_0 \geq 0$, where γ_0^2 is a limited positive number, then $\lim_{t\to\infty} e(t) = 0$.

The MARS system will be stable.

Finally, the equation of $\hat{\omega}$ can be achieved as:

$$\hat{\omega} = \int_0^t k_1(x_1\hat{x}_2 - x_2 x_1) dt + k_2(x_1\hat{x}_2 - x_2 x_1) + \hat{\omega}_{(0)} \qquad (49)$$

Where $k_1, k_2 \geq 0$

Replacing x with i :

$$\hat{\omega} = \int_0^t k_1(i_{ds}\hat{i}_{qs} - i_{qs}i_{ds} - \frac{\psi_r}{L_d}(i_{qs} - \hat{i}_{qs})) dt + k_2(i_{ds}\hat{i}_{qs} - i_{qs}i_{ds} - \frac{\psi_r}{L_d}(i_{qs} - \hat{i}_{qs})) + \hat{\omega}_{(0)} \qquad (50)$$

In the equation (50), $\hat{i}_{ds}$, $\hat{i}_{qs}$ can be calculated through the adjustable model, i_{ds}, i_{qs} can be obtained by the transformation of the measured stator currents.

The rotor position can be obtained by integrating the estimated speed:

$$\hat{\theta} = \int_0^t \hat{\omega} dt \qquad (51)$$

The MRAS scheme is illustrated in Figure 3.

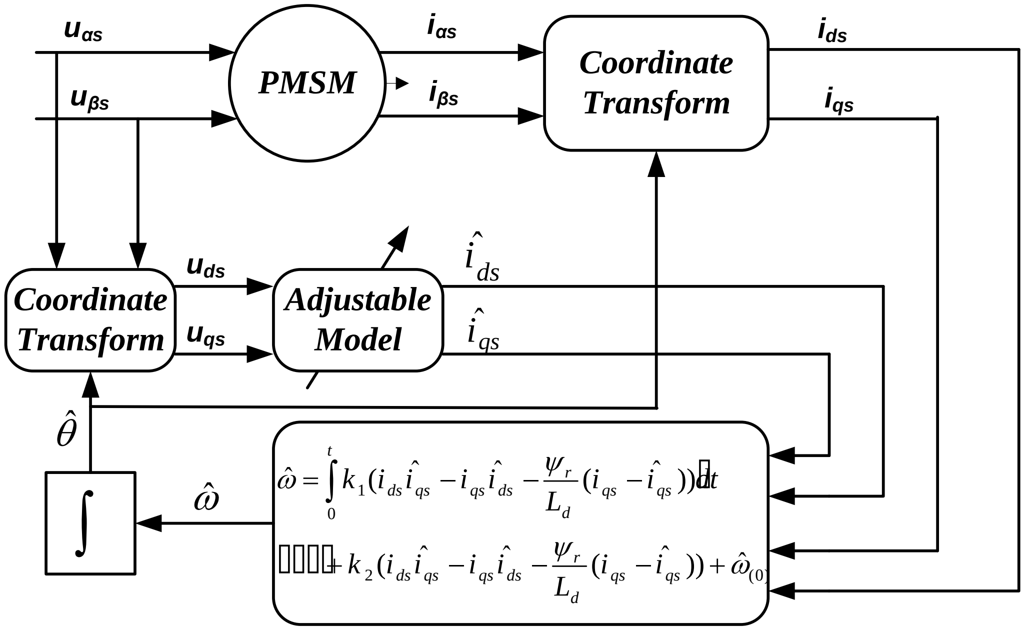

Figure 3. Control block scheme of MRAS

B. Observer-Based Estimators

Observer methods use instead of the reference model the real motor. The observer is the adaptive model with a constantly updated gain matrix ***K*** which is selected by choosing the eigenvalues in that way, that the system will be stable and that the transient of the system will be dynamically faster than the PM machine [29].

1) Luenberger Observer

A full order state observer with measureable estimated state variables, generally stator current, and not measurable variables like rotor flux linkages, back-EMF and rotor speed can be described in the form of state space equations for control of time invariant systems [29]:

$$\begin{aligned} \dot{\underline{x}} &= A\underline{x} + B\underline{u} \\ \underline{y} &= C\underline{x} \end{aligned} \qquad (52)$$

where ***A*** is the state matrix of the observer a function of the estimated rotor speed, ***B*** the input matrix and ***C*** output matrix.

In the following example the estimation algorithm observer based on back-EMF in α-β frame is considered. With the assumption that the back-EMF vector has the following form:

$$\begin{aligned} \underline{e} &= \begin{bmatrix} e_{\alpha s} \\ e_{\beta s} \end{bmatrix} \\ &= \{(L_d - L_q)(\omega_r i_{ds} - p i_{qs}) + \omega_r \psi_r\} \begin{bmatrix} -\sin\theta \\ \cos\theta \end{bmatrix} \end{aligned} \qquad (53)$$

and that electrical systems time constant is much smaller than the mechanical one. ω_r is regarded as a constant parameter. The linear state equation can be described as follows [26, 28, and 29]:

$$\frac{d}{dt}\begin{bmatrix} \underline{i}_{\alpha\beta s} \\ \underline{e}_{\alpha\beta s} \end{bmatrix} = A \begin{bmatrix} \underline{i}_{\alpha\beta s} \\ \underline{e}_{\alpha\beta s} \end{bmatrix} + B\,\underline{u}_{\alpha\beta s} + W \qquad (54)$$

$$\underline{i}_{\alpha\beta s} = C.\begin{bmatrix} \underline{i}_{\alpha\beta s} \\ \underline{e}_{\alpha\beta s} \end{bmatrix} \qquad (55)$$

Where,

$$\underline{i}_{\alpha\beta s} = [i_{\alpha s} \;\; i_{\beta s}]^T,\; \underline{e}_{\alpha\beta s} = [e_{\alpha s} \;\; e_{\beta s}]^T$$

$$A = \frac{1}{L_d}\begin{bmatrix} -R_s & -\omega_r(L_d - L_q) & -1 & 0 \\ \omega_r(L_d - L_q) & -R_s & 0 & -1 \\ 0 & 0 & 0 & -\omega_r \\ 0 & 0 & \omega_r & 0 \end{bmatrix}$$

$$B = \frac{1}{L_d}\begin{bmatrix} 1 & 0 \\ 0 & 1 \\ 0 & 0 \\ 0 & 0 \end{bmatrix},\; C = \begin{bmatrix} 1 & 0 & 0 & 0 \\ 0 & 1 & 0 & 0 \end{bmatrix}$$

$$W = (L_d - L_q)(\omega_r \dot{i}_{ds} - \dot{i}_{qs})\begin{bmatrix} -\sin\theta \\ \cos\theta \end{bmatrix}$$

The term W is the unknown linearization error and appears only, when i_{ds} or i_{qs} is changing.

The state equation of the Luenberger observer can be written as:

$$\frac{d}{dt}\begin{bmatrix} \hat{\underline{i}}_{\alpha\beta s} \\ \hat{\underline{e}}_{\alpha\beta s} \end{bmatrix} = \hat{A}\begin{bmatrix} \underline{i}_{\alpha\beta s} \\ \underline{e}_{\alpha\beta s} \end{bmatrix} + B\begin{bmatrix} u_{\alpha\beta s} \\ u_{\alpha\beta s} \end{bmatrix} + K(\underline{i}_{\alpha\beta s} - \hat{\underline{i}}_{\alpha\beta s}) \qquad (56)$$

$$\hat{\underline{i}}_{\alpha\beta s} = C.\begin{bmatrix} \hat{\underline{i}}_{\alpha\beta s} \\ \hat{\underline{e}}_{\alpha\beta s} \end{bmatrix} \qquad (57)$$

Where ^ denotes estimated values. $\hat{A}$ is a function of the rotor speed. Therefore the speed ω_r must also be estimated. The estimated speed can be calculated with a *PI*-controller which has the form of equation (58).

$$\hat{\omega}_r = k_p(e_{\alpha s}\varepsilon_\alpha - \hat{e}_{\beta s}\varepsilon_\beta) + k_i\int(e_{\alpha s}\varepsilon_\alpha - \hat{e}_{\beta s}\varepsilon_\beta)\,dt \qquad (58)$$

Where k_p and k_i are proportional and integral gain constants respectively, $\varepsilon_\alpha = i_{\alpha s} - \hat{i}_{\alpha s}$ and $\varepsilon_\beta = i_{\beta s} - \hat{i}_{\beta s}$ are the *α-β* axis current errors respectively. For obtaining error dynamic (34) can be used. It can be seen, that the dynamics are described by the eigenvalues of $A - KC$. To determine the stability of the error dynamics of the observer it can be used Popov's super stability theorem or Lyapunov's stability theorem which gives a sufficient condition for the uniform asymptotic stability of non-linear system by using the Lyapunov function *V*. A sufficient condition for the uniform asymptotic stability is that the derivate of *V* is negative definite. If the observer gain ***K*** is chosen that $(A - KC)^T$ is negative semi-definite, then the speed observer will be stable [29].

Further literature in flux-based observer can be found in [31, 32].

Systems with a Luenberger observer generally have a better performance than MRAS based Systems. MRAS based systems have a higher error in the estimated values. Furthermore, the Luenberger approach has a less tendency to oscillate in the range of low speed and need in comparison with the kalman Filter method less computation time and memory requirement [29, 33].

2) Reduced Order Observer

Paper [34] is included on the idea of the reduced order observer. The design method considers a general dynamic system in the form of equation (52).

Where the pair **(*C, A*)** is observable. If the output ***y*** can be written as a combination of the state vector as:

$$y = C_1 x_1 + C_2 x_2 \; ; \quad \det(C_2) \neq 0 \tag{59}$$

Then, it is sufficient to design an observer for the partial state x_1. If $\hat{x}_1$ is the estimate of x_1, the partition x_2 of the state vector can be calculated as:

$$\hat{x}_2 = C_2^{-1}(y - C_1 x_1) \tag{60}$$

The reduced order observer allows for order reduction, is simpler to implement and the state partition x_2 is found using the algebraic equation (60).

The design methodology of the reduced order observer requires transformation of the original system to the form:

$$\dot{x}_1 = A_{11}x_1 + A_{12}y + B_1 u \tag{61}$$

$$\dot{y} = A_{21}x_1 + A_{22}y + B_2 u \tag{62}$$

A new variable x' is introduced:

$$x' = x_1 + L_1 y \tag{63}$$

where L_1 is a nonsingular gain matrix. After the differentiation and algebraic manipulation of (63), the following form is obtained:

$$\dot{x}' = (A_{11} + L_1 A_{21})x' + (A_{12} + L_1 A_{22} - A_{11}L_1 - L_1 A_{21} L_1)y + (B_1 + L_1 B_2)u \tag{64}$$

An observer for x' is designed in the form:

$$\dot{\hat{x}}' = (A_{11} + L_1 A_{21})\hat{x}' + (A_{12} + L_1 A_{22} - A_{11}L_1 - L_1 A_{21} L_1)y + (B_1 + L_1 B_2)u \tag{65}$$

After subtraction, the dynamics of the mismatch is:

$$\dot{\bar{x}}' = (A_{11} + L_1 A_{21})\bar{x}' \tag{66}$$

With the known matrices A_{11} and A_{21}, the gains in L_1 can be selected to obtain desired eigenvalues. Therefore, the mismatch tends to zero with the desired rate of convergence. Once $\hat{x}'$ has been estimated, the state partition x_1 follows from (63) and x_2 is calculated using (60).

Further literature in reduced order observer can be found in [35-37].

3) Sliding Mode Observer

In [38, 39] present a sliding mode observer (SMO) for the estimation of the EMFs and the rotor position of the PMSM. The observer is constructed based on the full PMSM model in the stationary reference frame. The proposed sliding mode observer is developed based on the equations of the PMSM with respect to the currents and EMFs:

$$pe_{\alpha s} = -\omega e_{\beta s} \tag{67}$$

$$pe_{\beta s} = \omega e_{\alpha s} \tag{68}$$

$$pi_{\alpha s} = -\frac{R_s}{L} i_{\alpha s} - \frac{1}{L} e_{\alpha s} + \frac{1}{L} v_{\alpha s} \tag{69}$$

$$pi_{\beta s} = -\frac{R_s}{L} i_{\beta s} - \frac{1}{L} e_{\beta s} + \frac{1}{L} v_{\beta s} \tag{70}$$

The voltages $v_{\alpha s}$, $v_{\beta s}$ and currents $i_{\alpha s}$, $i_{\beta s}$ are measured and considered known. In the observer, a speed estimate is used according to (71); the speed estimate is considered different than the real speed (note that $\Delta\omega$ is unknown).

$$\hat{\omega} = \omega + \Delta\omega \tag{71}$$

The observer equations are:

$$p\hat{e}_{\alpha s} = -(\omega + \Delta\omega) e_{\beta s} + l_{11} u_{\alpha s} \tag{72}$$

$$p\hat{e}_{\beta s} = (\omega + \Delta\omega) e_{\alpha s} + l_{22} u_{\beta s} \tag{73}$$

$$p\hat{i}_{\alpha s} = -\frac{R_s}{L} i_{\alpha s} - \frac{1}{L} \hat{e}_{\alpha s} + \frac{1}{L} v_{\alpha s} - \frac{1}{L} u_{\alpha s} \tag{74}$$

$$p\hat{i}_{\beta s} = -\frac{R_s}{L} i_{\beta s} - \frac{1}{L} \hat{e}_{\beta s} + \frac{1}{L} v_{\beta s} - \frac{1}{L} u_{\beta s} \tag{75}$$

where the switch (sliding mode) controls $u_{\alpha s}$, $u_{\beta s}$ are:

$$\begin{matrix} u_{\alpha s} = M \cdot sign(s_\alpha) \\ u_{\beta s} = M \cdot sign(s_\beta) \end{matrix} ; \quad \begin{matrix} s_\alpha = \hat{i}_{\alpha s} - i_{\alpha s} \\ s_\beta = \hat{i}_{\beta s} - i_{\beta s} \end{matrix} \tag{76}$$

Note that M is a design gain, $M > 0$; l_{11} and l_{22} are design parameters. After the original equations (67) to (70) are subtracted from (72) to (75), system is obtained by following equations:

$$p\bar{e}_{\alpha s} = -\omega \bar{e}_{\beta s} - \Delta\omega \hat{e}_{\beta s} + l_{11} u_{\alpha s} \tag{77}$$

$$p\bar{e}_{\beta s} = \omega \bar{e}_{\alpha s} - \Delta\omega \hat{e}_{\alpha s} + l_{22} u_{\beta s} \tag{78}$$

$$\dot{s}_\alpha = -\frac{R_s}{L} s_\alpha + \frac{1}{L} \bar{e}_{\alpha s} - \frac{1}{L} u_{\alpha s} \tag{79}$$

$$\dot{s}_\beta = -\frac{R_s}{L} s_\beta + \frac{1}{L} \bar{e}_{\beta s} - \frac{1}{L} u_{\beta s} \tag{80}$$

In the last two equations (79) and (80), note that if the sliding mode gain M is high enough, the manifolds s_α, s_β and their time derivatives have opposite signs. As a result, the manifolds tend to zero and sliding mode occurs; i.e. $s_\alpha \rightarrow 0$ and $s_\beta \rightarrow 0$. Once sliding mode starts, s_α, s_β and their derivatives are identically equal to zero. The equivalent controls are:

$$\begin{matrix} u_{\alpha s,eq} = \bar{e}_{\alpha s} \\ u_{\beta s,eq} = \bar{e}_{\beta s} \end{matrix} \tag{81}$$

In order to study the behavior of the mismatches $\bar{e}_{\alpha s}$, $\bar{e}_{\beta s}$, the terms $u_{\alpha s}$ and $u_{\beta s}$ are replaced with the equivalent controls in the first two equations of (77) and (78). The resulting dynamics of the EMF mismatches is:

$$p\bar{e}_{\alpha s} = -\omega \bar{e}_{\beta s} - \Delta\omega \hat{e}_{\beta s} + l_{11}\bar{e}_{\alpha s} \quad (82)$$

$$p\bar{e}_{\beta s} = \omega \bar{e}_{\alpha s} - \Delta\omega \hat{e}_{\alpha s} + l_{22}\bar{e}_{\beta s} \quad (83)$$

Next, select the candidate Lyapunov function which is positive definite, ***V***> 0.

$$V = \frac{1}{2}(\bar{e}_{\alpha s}^{\,2} + \bar{e}_{\beta s}^{\,2}) \quad (84)$$

After differentiation, the expression of $\dot{V}$ is:

$$\dot{V} = \dot{\bar{e}}_{\alpha s}\bar{e}_{\alpha s} + \dot{\bar{e}}_{\beta s}\bar{e}_{\beta s} \quad (85)$$

After replacing the derivatives from (82) and (83), this becomes:

$$\dot{V} = l_{11}\bar{e}_{\alpha s}^{\,2} + l_{22}\bar{e}_{\beta s}^{\,2} - \Delta\omega \hat{e}_{\beta s}\bar{e}_{\alpha s} + \Delta\omega e_{\alpha s}\bar{e}_{\beta s} \quad (86)$$

If $l_{11} = l_{22} = -k$ where $k > 0$, the derivative of V is:

$$\dot{V} = -k(\bar{e}_{\alpha s}^{\,2} + \bar{e}_{\beta s}^{\,2}) + \Delta\omega(\hat{e}_{\beta s}\bar{e}_{\alpha s} - e_{\alpha s}\bar{e}_{\beta s}) \quad (87)$$

Equation (87) will be used to study the convergence of the observer. Note that $\dot{V} < 0$ If $\Delta\omega = 0$ and the observer is asymptotically stable. There are two terms in (87): the first one is always negative (and can be increased using the design parameter ***k***) while the second one has unknown sign. As long as the mismatches $\bar{e}_{\alpha s}$ and $\bar{e}_{\beta s}$ are significant, the first term overcomes the second and $\dot{V}$ is negative (as a result, function V decays). The Lyapunov function stops decaying when $\dot{V} = 0$ and this is equivalent to:

$$k(\bar{e}_{\alpha s}^{\,2} + \bar{e}_{\beta s}^{\,2}) = \Delta\omega(\hat{e}_{\beta s}\bar{e}_{\alpha s} - e_{\alpha s}\bar{e}_{\beta s}) \quad (88)$$

Since the mismatches $\bar{e}_{\alpha s}$, $\bar{e}_{\beta s}$ should be of the same order of magnitude, using the notation $m\bar{e}_{\alpha s} = \bar{e}_{\beta s}$ (where ***m*** is unknown), equation (88) is manipulated to give the value of the mismatch $\bar{e}_{\alpha s}$ at which the function V stops decaying:

$$\bar{e}_{\alpha s} = \Delta\omega \frac{m\,\hat{e}_{\beta s} - e_{\alpha s}}{k(1+m^2)} \quad (89)$$

The Lyapunov function settles to the vicinity given by the mismatch in (89), and the size of this vicinity (and the mismatch) can be reduced by increasing k (which is a design parameter). The analysis shows that the influence of the speed mismatch $\Delta\omega$ (caused by the speed observer) can be made irrelevant by proper design of the SM observer gains; the mismatch between the real and estimated EMFs can be made as small as desired according to (89). Once the EMFs have been found, the rotor position is computed directly with:

$$\hat{\theta} = \tan^{-1}\left(-\frac{\hat{e}_{\alpha s}}{\hat{e}_{\beta s}}\right) \quad (90)$$

Further literature in sliding mode observer (SMO) can be found in [40-43].

The main difference between the Luenberger and the Sliding mode observer (SMO) lies in the observer structure. The SMO uses a sign-function of the estimation error instead of the linear value as correction feedback [44].

4) Kalman Filter

The kalman filter is in principle a state observer that establishes the approximation for the state variables of a system, by minimization of the square error, subjected at both its input and output to random disturbances. If the dynamic system of which the state is being observed is non-linear, then the kalman filter is called an extended kalman filter (EKF). The EKF is basically a full-order stochastic observer for the recursive optimum state estimation of a nonlinear dynamical system in real time by using signals that are in noisy environments. The EKF can also be used for unknown parameter estimation or joint state [45]. The linear stochastic systems are described by relations [7]:

$$\dot{x}(t) = Ax(t) + Bu(t) + w(t)\,; \quad x(t_o) = x_o \qquad (91)$$

$$y(t) = Cx(t) \qquad (92)$$

$$z(t) = y(t) + \nu(t) \qquad (93)$$

Where:

x, y, u, A, B, C have the significance known from deterministic system; $w(t)$ represents the vector of disturbances applied at the system input; $z(t)$ is the vector of the measurable outputs, affected by the random noise $\nu(t)$.

It can be considered that, besides the input disturbances, vector $w(t)$ includes some uncertainties referring to the process model. It will be assumed that the vector functions $w(t)$ and $\nu(t)$ are not correlated and zero-mean stochastic processes. From statistic point of view, the stochastic processes $w(t)$ and $\nu(t)$ are characterized by the covariance matrices *Q* and *R*, respectively. It is further assumed that the initial state x_o is a vector of random variables, of mean $\bar{x}_o$ and covariance P_0, not correlated with the stochastic processes $w(t)$ and $\nu(t)$ over the entire interval of estimation.

The covariance matrices *Q*, *R*, P_0 characterizing the noise sources of system (94)-(96) are, by definition, symmetrical and positively semi-definite, of dimensions (*n x n*), (*m x m*) and (*n x n*) respectively, where n and m represent the number of state and output variables, respectively.

For linear time invariant systems, the following relations of recurrent computation describe the general form of the kalman filter implementation algorithm:

$$K_k = P_{k|k-1} C^T (C P_{k|k-1} C^T + R)^{-1} \qquad (94)$$

$$\hat{x}_{k|k} = x_{k|k-1} + K_k (y_k - C\hat{x}_{k|k-1}) \qquad (95)$$

$$P_{k|k} = (I_n - K_k C) P_{k|k-1} \qquad (96)$$

$$\hat{x}_{k+1|k} = A_d x_{k|k} + T_s B u_k \qquad (97)$$

$$P_{k+1|k} = A_d P_{k|k} A_d^{\,T} + Q \qquad (98)$$

Where T_s represents the sampling period and $\boldsymbol{A_d}$ is the matrix of the discrete linearized system:

$$A_d = I_n + T_s A \qquad (99)$$

In these relationships, the (*n x m*) matrix ***K*** represents the kalman gain; ***P*** represents the covariance state matrix and $\boldsymbol{I_n}$ is the (*n x n*) unit matrix. In the recurrent computation relationships, the subscript index notations of type ***k/k-1*** show that the respective quantities (state vectors or their covariance matrices) are computed for sample ***k***, using the values of similar quantities from the previous sample.

For non-linear stochastic systems, the dynamic state model is described by the following expressions:

$$\dot{x}(t) = f(x(t), u(t), t) + w(t) \qquad (100)$$

$$y(t) = h(x(t), t) \qquad (101)$$

$$z(t) = h(x(t), t) + \nu(t) \qquad (102)$$

where ***f*** and ***h*** are (*n x 1*) and (*m x 1*) function vectors, respectively. The ***A*** and ***C*** matrices of the EKF structure are dependent now upon the state of the system and are determined by:

$$A(\hat{x}(t),t) = \frac{\partial f\,(x(t),u(t),t)}{\partial x^{T}(t)}\Big|_{x(t)=\hat{x}(t)} \qquad (103)$$

$$C(\hat{x}(t),t) = \frac{\partial h(x(t),t)}{\partial x^{T}(t)}\Big|_{x(t)=\hat{x}(t)} \qquad (104)$$

Additionally to the fact that matrices ***A*** and ***c*** have now become dependent on the state of the system, the algorithm suffers some further changes, which affect relationships (95) and (97), now expressed as:

$$\hat{x}_{k|k} = x_{k|k-1} + K_k[y_k - h(\hat{x}_{k|k-1})] \qquad (105)$$

$$\hat{x}_{k+1|k} = x_{k|k} + T_s f\,(\hat{x}(t),u(t)) \qquad (106)$$

The kalman filter algorithm is initiated by adopting adequate values for the covariance matrix of the initial state $P_0 = P_{0|-1}$, as well as for the weighting matrices ***Q*** and ***R***, the latter two being constant during the estimation.

EKF is known for its high convergence rate, which significantly improves transient performance. However, the long computation time is a main drawback of the EKF [45]. Although last-generation floating-point digital signal processors can easily overcome the EKF real-time calculations [46], this is not suitable for low-cost PMSM applications. Moreover, long computation requirements disturb other program service routines such as fault diagnosis or custom programs installed in products. [47] presents the optimal two-stage kalman estimator (OTSKE) which is composed of two parallel filters: a full order filter and another one for the augmented state. This estimator has the advantage of reducing the computational complexity compared to the classical EKF.

The application of the EKF in the sensorless PMSM drive system will be increased a lot [29, 48]. The main steps for a speed and position sensorless PMSM drive implementation using a discredited EKF algorithm can be found in [45, 48-51].

3.2 Saliency and Signal Injection Methods

In signal injection methods, the feature of salient-pole PMSMs such that the inductance varies with the rotor position is used. High frequency voltage or current signal is injected on the top of the fundamental, and signal processing (vector filters with inevitable time delay) is employed to extract currents harmonics that contain rotor position. Thus, the position can be estimated even at standstill and low speeds, robustly to parameter variations [52]. For wide speed range, hybrid methods are used [53]. High frequency signal injection techniques, Figure 4, are considered to be superior to other sensorless control schemes of ac machines for low and zero speed operation.

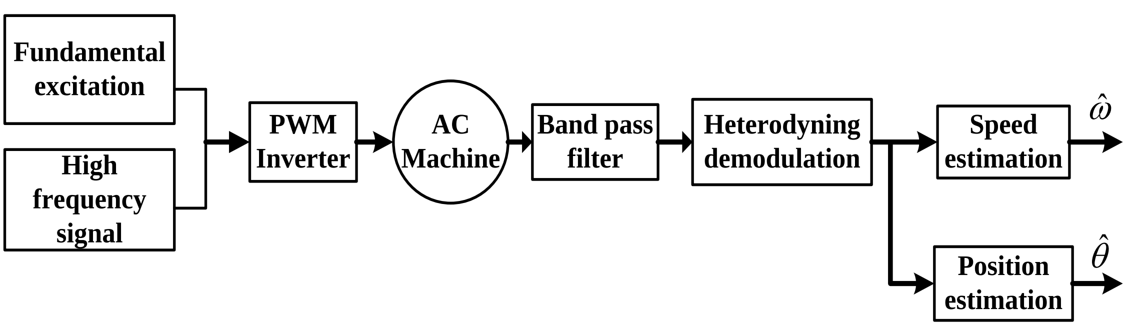

Figure 4. High frequency signal injection block diagram

Based on the injection direction of the excitation signal, the high frequency injection schemes could be classified as rotating injection method, in which the carrier signal is a rotating sinusoidal signal in the stationary reference frame; pulsating injection method, in which an ac voltage signal is injected on the estimated rotor d-axis, rotating with the rotor and the rotor position offset could be observed from the high frequency component of the estimated q-axis current. However, the drive efficiency of the schemes is hard to be accessed and the development of the sensorless strategies suffers the unknown nonlinearity of the model [54].

Other methods are based on the signal processing of PWM excitation without signal injection. The SV-PWM waveforms provide sufficient excitation to extract the position signal from the stator current. These methods are: Indirect Flux detection by On-line Reactance Measurement (INFORM) method, and methods based on the measurements of *di/dt* of the stator currents induced by SV-PWM. Typically, the injected signal is a sinusoidal type. To eliminate the time delay introduced by filters, a new square wave signal injection method is proposed, based only on the measurement of the corresponding induced stator current variations, which leads to high dynamics and robust position estimation [52].

Magnetic saliency methods are relatively complicated for real time implementation and are less portable from one machine to another; however, they work well at low speed. The rotor position of the PMSM can also be estimated at standstill; as a result, the motor can be started with the correct rotor position from the beginning of the motion [38].

Further literatures which use the magnetic saliency methods can be found in [55-58].

3.3 Artificial Intelligence Methods

Artificial intelligence describe neural network (NN), fuzzy logic based systems (FLS) and fuzzy neural networks (FNN). The use of artificial intelligence (AI) to identify and control nonlinear dynamic systems has been proposed because they can approximate a wide range of nonlinear functions to any desired degree of accuracy [59]. Moreover, they have been the advantages of immunity from input harmonic ripples and robustness to parameter variations. However, ANN controller synthesis requires design of the control structure which includes selecting the neural network structure, weight coefficients and activation function. The selection of neural structure as the initial step is done by trial and error method since there is no proper procedure for this [60]. The complex of the selected neural network structure is a compromise between the high quality of control robustness and the possibility of control algorithm calculation in real time. This gives rise to inaccuracies [60]. Recently, there have been some investigations into the application of AI to power electronics and ac drives, including speed estimation [60-63].

Paper [64] presents a robust control strategy with NN flux estimator for a position sensorless SPMSM drive. In the proposed algorithm stator flux is estimated from stationary *α-β* axis stator currents and speed error, E_ω. An equivalent Recurrent Neural Network (RNN) is then proposed which results in the following matrix equation:

$$\begin{bmatrix}\psi_{\alpha s}(k+1)\\ \psi_{\beta s}(k+1)\end{bmatrix}=\begin{bmatrix}W_{11} & 0\\ 0 & W_{22}\end{bmatrix}\begin{bmatrix}\psi_{\alpha s}(k)\\ \psi_{\beta s}(k)\end{bmatrix}+\begin{bmatrix}W_{13}\\ W_{23}\end{bmatrix}i_{\alpha s}(k)+\begin{bmatrix}W_{14}\\ W_{24}\end{bmatrix}i_{\beta s}(k)+\begin{bmatrix}W_{15}\\ W_{25}\end{bmatrix}E_w(k) \quad (107)$$

where, W_{11}, W_{13}, W_{22}, W_{23}, W_{14} etc. are the weights of the RNN.

The estimated stator flux using RNN is used to find out the rotor position as following:

$$\theta=\delta+\gamma \quad (108)$$

Where, γ is the flux angle, and δ is the torque angle. Where $\gamma = \tan^{-1}(\frac{\psi_{\beta s}}{\psi_{\alpha s}})$

4. Parameter Adaptation

Motion-sensorless PMSM drives may have an unstable operating region at low speeds. Since the back electromotive force (EMF) is proportional to the rotational speed of the motor, parameter errors have a relatively high effect on the accuracy of the estimated back EMF at low speeds [65]. Improper observer gain selections may cause unstable operation of the drive even if the parameters are accurately known [66].

In practice, the stator resistance varies with the winding temperature during the operation of the motor, so there is often a mismatch between the actual winding resistance and its corresponding value in the model used for speed estimation. This may lead not only to a substantial speed estimation error but to instability as well.

Parameter variation not only degrades the control performance but also causes an error in the estimated position [67]. As consequence, numerous online schemes for parameter identification have been proposed, recently [65-69].

5. Conclusion

Recently, permanent magnet synchronous motor (PMSM) drives are replacing classic dc and induction machine drives in a variety of industrial applications. PMSM drive research has been concentrated on the elimination of the mechanical sensors at the motor shaft without deteriorating the dynamic performances of the drive. Many advantages of sensorless ac drives such as reduced hardware complexity, low cost, reduced size, cable elimination, increased noise immunity, increased reliability and decreased maintenance.in this paper, a review of different speed and rotor position estimation schemes of PMSM drives has been introduced. Each method has its advantages and disadvantages. Although numerous schemes have been proposed for speed and rotor position estimation, many factors remain important to evaluate their effectiveness. Among them are steady state error, dynamic behavior, noise sensitivity, low speed operation, parameter sensitivity, complexity, and computation time. In particular, zero-speed operation with robustness against parameter variations yet remains an area of research for speed sensorless control.

As a final comment, each speed estimation method of sensorless application requires a specific design, which takes into consideration the required performance, the available hardware and the designer skills.

References:

[1] S. Yu, Z. Yang, S. Wang and K. Zheng, "Sensorless Adaptive Backstepping Speed Tracking Control of Uncertain Permanent Magnet Synchronous Motors", in Conf. Rec., IEEE-ISCAA, June 2010, pp. 1131-1135.

[2] Q. Gao, S. Shen, and T. Wang, "A Novel Drive Strategy for PMSM Compressor", in Conf. Rec., IEEE-ICECE, June 2010, pp. 3192 – 3195.

[3] Z. Peroutka, K. Zeman, F. Krus, and F. Kosten, "New Generation of Trams with Gearless Wheel PMSM Drives: From Simple Diagnostics to Sensorless Control", in IEEE Conf. Rec., 14th International Power Electronics and Motion Control Conference EPE-PEMC, September 2010, pp. 31-36.

[4] H. Peng, H. Lei, and M. Chang-yun, "Research on Speed Sensorless Backstepping Control of Permanent Magnet Synchronous Motor", in Conf. Rec., IEEE-ICCASM, October 2010, Vol. 15, pp. 609-612.

[5] J. Sung Park, S. Hun Lee, C. Moon, and Y. Ahn Kwon, "State Observer with Stator Resistance and Back-EMF Constant Estimation for Sensorless PMSM", IEEE Region 10 Conference, TENCON 2010, November 2010, pp. 31-36.

[6] T. J. Vyncke, R. K. Boel and J. A. A. Melkebeek, "Direct Torque Control of Permanent Magnet Synchronous Motors – An Overview", 3rd IEEE Benelux Young Researchers Symposium in Electrical Power Engineering, April 2006, pp. 1-5.

[7] V. Comnac, M. N. Cirstea, F. Moldoveanu, D. N. Ilea, and R. M. Cernat, "Sensorless Speed and Direct Torque Control of Interior Permanent Magnet Synchronous Machine Based on Extended Kalman Filter", in Proc. of the IEEE-ISIE Conf., Vol. 4, November 2002, pp. 1142-1147.
[8] M. S. Merzoug, and F. Naceri, "Comparison of Field-Oriented Control and Direct Torque Control for Permanent Magnet Synchronous Motor (PMSM)", in World Academy of Science, Engineering and Technology, Vol. 48, 2008, pp. 299-304.
[9] Y. Xu, and Y. Zhong, "Speed Sensorless Direct Toque Control of Interior Permanent Magnet Synchronous Motor Drive Based on Space Vector Modulation", in Conf. Rec., IEEE-ICECE, June 2010, pp. 4226-4230.
[10] J. Arellano-Padilla, C. Gerada, G. Asher, and M. Sumner, "Inductance Characteristics of PMSMs and their Impact on Saliency-based Sensorless Control", in IEEE Conf. Rec., 14th International Power Electronics and Motion Control Conference EPE-PEMC, September 2010, pp. 1-9.
[11] K. Jezernik, R. Horvat, "High Performance Control of PMSM ", in Conf. Rec., IEEE-SLED, July 2010, pp. 72-77.
[12] S. Sumita, K. Tobari, S. Aoyagi, and D. Maeda, "A Simplified Sensorless Vector Control Based on the Average of the DC Bus Current", in Conf. Rec., IEEE-IPEC, June 2010, pp.3035-3040.
[13] R. Mustafa, Z. Ibrahim and J. Mat Lazi, "Sensorless Adaptive Speed Control for PMSM Drives", in IEEE Conf. Rec., 4th International Power Engineering and Optimization Conf., PEOCO'10, June 2010, pp. 511-516.
[14] O. Benjak, and D. Gerling, "Review of Position Estimation Methods for IPMSM Drives Without a Position Sensor Part I: Nonadaptive Methods", in Conf. Rec., IEEE-ICEM, September 2010, pp. 1-6.
[15] M. A. Jabbar, M. A. Hoque, and M. A. Rahman, "Sensorless Permanent Magnet Synchronous Motor Drives", IEEE Canadian Conference on Electrical and Computer Engineering, CCECE'97, Vol. 2, May 1997, pp. 878-883.
[16] J. P. Johnson, M. Ehsani, and Y. Guzelgunler, "Review of Sensorless Methods for Brushless DC", in Conf. Rec., IEEE-IAS'99, Annual Meeting, Vol. 1, October 1999, pp. 143-150.
[17] S. Kondo, A. Takahashi and T. Nishida, "Armature Current Locus Based Estimation Method of Rotor Position of Permanent Magnet Synchronous Motor without Mechanical Sensor", in Conf. Rec., IEEE-IAS'95, Annual Meeting, Vol. 1, October 1995, pp. 55-60.
[18] L. Yongdong, and Z. Hao, "Sensorless Control of Permanent Magnet Synchronous Motor – A Survey", in Conf. Rec., IEEE-VPPC'08, September 2008, pp. 1-8.
[19] T. D. Batzel, and K. Y. Lee, "Electric Propulsion with the Sensorless Permanent Magnet Synchronous Motor: Model and Approach", IEEE Transactions on Energy Conversion, Vol. 20, No. 4, December 2005, pp. 818-825.
[20] T. Kim, H. Lee, and M. Ehsani, "State of the Art and Future Trends in Position Sensorless Brushless DC Motor/Generator Drives", Proc. of the 31th Annual Conference of the IEEE-IECON, November 2005, pp. 1718-1725.
[21] N. Bekiroglu, S. Ozcira, "Observerless Scheme for Sensorless Speed Control of PMSM Using Direct Torque Control Method with LP Filter", Advances in Electrical and Computer Engineering (AECE), Vol. 10, No. 3, August 2010, pp. 78-83.
[22] D. Yousfi, A. Halelfadl, and M. EI Kard, "Sensorless Control of Permanent Magnet Synchronous Motor", in Conf. Rec., IEEE-ICMCS'09, April 2009, pp. 341-344.
[23] D. Paulus, J.-F. Stumper, P. Landsmann, and R. Kennel, "Robust Encoderless Speed Control of a Synchronous Machine by direct Evaluation of the Back-EMF Angle without Observer", in Conf. Rec., IEEE-SLED, July 2010, pp. 8-13.
[24] S. Shimizu, S. Morimoto, and M. Sanada, "Sensorless Control Performance of IPMSM with Over-modulation Range at High Speed", in Conf. Rec., IEEE-ICEMS'09, November 2009, pp. 1-5.
[25] F. Genduso, R. Miceli, C. Rando, and G. R. Galluzzo, "Back EMF Sensorless-Control Algorithm for High-Dynamic Performance PMSM", IEEE Transactions on Industrial Electronics, Vol. 57, No. 6, June 2010, pp. 2092-2100.
[26] Z. Chen, M. Tomita, S. Doki, and S. Okuma, "An Extended Electromotive Force Model for Sensorless Control of Interior Permanent Magnet Synchronous Motors", IEEE Transactions on Industrial Electronics, Vol. 50, No. 2, April 2003, pp. 288-295.

[27] S. Morimoto, K. Kawamoto, M. Sanada, and Y. Takeda, "Sensorless Control Strategy for Salient-Pole PMSM Based on Extended EMF in Rotating Reference Frame", IEEE Transactions on Industry Applications, Vol. 38, No. 4, July/August 2002, pp. 1054-1061.

[28] S. Ichikawa, Z. Chen, M. Tomita, S. Doki, and S. Okuma, "Sensorless Control of an Interior Permanent Magnet Synchronous Motor on the Rotating Coordinate Using an Extended Electromotive Force", Proc. of the 27th Annual Conference of the IEEE-IECON, Vol. 3, November/December 2001, pp. 1667-1672.

[29] O. Benjak, D. Gerling, "Review of Position Estimation Methods for IPMSM Drives without a Position Sensor Part II: Adaptive Methods", in Conf. Rec., IEEE-ICEM, September 2010, pp. 1-6.

[30] Y. Shi, K. Sun, H. Ma, and L. Huang, "Permanent Magnet Flux Identification of IPMSM based on EKF with Speed Sensorless Control", Proc. of the 36th Annual Conference of the IEEE-IECON, November 2010, pp. 2252-2257.

[31] T. F. Chan, W. Wang, P. Borsje, Y. K. Wong, and S. L. Ho, "Sensorless permanent-magnet synchronous motor drive using a reduced-order rotor flux observer", Electric Power Applications, IET, Vol. 2, No. 2, March 2008, pp. 88-98.

[32] P. Vaclavek, and P. Blaha, "PMSM Position Estimation Algorithm Design based on the Estimate Stability Analysis", in Conf. Rec., IEEE-ICEMS'09, November 2009, pp. 1-5.

[33] B. S. Bhangu, and C. M. Bingham, "GA-tuning of Nonlinear Observers for Sensorless Control of Automotive Power Steering IPMSMs", in Conf. Rec., IEEE-VPPC, September 2005, pp. 772-779.

[34] M. Comanescu, and T. D. Batzel, "Reduced Order Observers for Rotor Position Estimation of Nonsalient PMSM", in Conf. Rec., IEEE-IEMDC'09, May 2009, pp. 1346-1351.

[35] D. Yousfi, A. Halelfadl, and M. EI Kard, "Review and Evaluation of Some Position and Speed Estimation Methods for PMSM Sensorless Drives ", in Conf. Rec., IEEE-ICMCS'09, April 2009, pp. 409-414.

[36] C. H. De Angelo, G. R. Bossio, J. A. Solsona, G. O. Garcia, and M. I. Valla, "Sensorless Speed Control of Permanent Magnet Motors Driving an Unknown Load", in Conf. Rec., IEEE-ISIE'03, Vol. 1, June 2003, pp. 617-620.

[37] S. Ichikawa, C. Zhiqian, M. Tomita, S. Doki, and S. Okuma, "Sensorless Control of an Interior Permanent Magnet Synchronous Motor on the Rotating Coordinate Using an Extended Electromotive Force", Proc. of the 27th Annual Conference of the IEEE-IECON, Vol. 3, November/December 2001, pp. 1667-1672.

[38] M. Comanescu, "Rotor Position Estimation of PMSM by Sliding Mode EMF Observer under improper speed", in Proc. of the IEEE-ISIE Conf., July 2010, pp. 1474-1478.

[39] M. Comanescu, "Cascaded EMF and Speed Sliding Mode Observer for the Nonsalient PMSM", Proc. of the 36th Annual Conference of the IEEE-IECON, November 2010, pp.792-797.

[40] M. Ezzat, J. de Leon, N. Gonzalez, and A. Gluminea, "Observer-Controller Scheme using High Order Sliding Mode Techniques for Sensorless Speed Control of Permanent Magnet Synchronous Motor", Proc. of the 49th Conference of the IEEE-CDC, December 2010, pp. 4012-4017.

[41] Y. Nan, and T. Zhang, "Research of Position Sensorless Control for PMSM Based on Sliding Mode Observer", 2nd international conference of the IEEE-ICISE, December 2010, pp. 5282-5285.

[42] L. Jun, W. Gang, and Y. JinShou, "A Study of SMO Buffeting Elimination in Sensorless Control of PMSM", in Proc. of the IEEE-WCICA Conf., July 2010, pp. 4948-4952.

[43] Zhang Niaona, Guo yibo and Zhang Dejiang, "Sliding Observer Approach for Sensorless Operation of PMSM Drive", in Proc. of the IEEE-WCICA Conf., July 2010, pp. 5809-5813.

[44] L. Jiaxi, Y. Guijie, and L. Tiecai, "A New approach to Estimated Rotor Position for PMSM Based on Sliding Mode Observer", in Conf. Rec., IEEE-ICEMS'07, October 2007, pp. 426-431.

[45] J. Jang, B. Park, T. Kim, D. M. Lee, and D. Hyun, "Parallel Reduced-Order Extended Kalman Filter for PMSM Sensorless Drives", Proc. of the 34th Annual Conference of the IEEE-IECON, November 2008, pp. 1326-1331.

[46] S. Bolognani, R. Oboe, and M. Zigliotto, "Sensorless Full-Digital PMSM Drive with EKF Estimation of Speed and Rotor Position", IEEE Transactions on Industrial Electronics, Vol. 46, No. 1, February 1999, PP. 184-191.

[47] A. Akrad, M. Hilairet, and D. Diallo, "Performance Enhancement of a Sensorless PMSM drive with Load Torque Estimation", Proc. of the 36th Annual Conference of the IEEE-IECON, November 2010, pp. 945-950.
[48] T. J. Vyncke, R. K. Boel, and J. A. A. Melkebeek, "On Extended Kalman Filters with Augmented State Vectors for the Stator Flux Estimation in SPMSMs", in Proc. of the Twenty-Fifth Annual IEEE-APEC Conf., February 2010, pp. 1711-1718.
[49] A. Titaouinen, F. Benchabane, o. Bennis, K. Yahia, and D. Taibi, "Application of AC/DC/AC Converter for Sensorless Nonlinear Control of Permanent Magnet Synchronous Motor", in Conf. Rec., IEEE-SMC, October 2010, pp. 2282-2287.
[50] F. Benchabane, A. Titaouine, o. Bennis, K. Yahia, and D. Taibi, "Systematic Fuzzy Sliding Mode Approach Combined With Extented Kalman Filter for Permanent Magnet Synchronous Motor control", in Conf. Rec., IEEE-SMC, October 2010, pp. 2169-2174.
[51] S. Carriere, S. Caux, M. Fadel, and F. Alonge, "Velocity sensorless control of a PMSM actuator directly driven an uncertain two-mass system using RKF tuned with an evolutionary algorithm", in Proc. of the IEEE-(EPE/PEMC) Conf., September 2010, pp. 213-220.
[52] G.-D. Andreescu and C. Schlezinger, "Enhancement Sensorless Control System for PMSM Drives Using Square-Wave Signal Injection", Proceedings of the International Symposium on Power Electronics, Electrical Drives, Automation and Motion (SPEEDAM), June 2010, pp. 1508-1511.
[53] D. Xiao, G. Foo, and M. F. Rahman, "A New Combined Adaptive Flux Observer with HF Signal Injection for Sensorless Direct Torque and Flux Control of Matrix Converter Fed IPMSM over a Wide Speed Range", IEEE Energy Conversion Congress and Exposition, ECCE'10, September 2010, pp. 1859-1866.
[54] Y. Wang, J. Zhu, Y. Guo, Y. Li, and W. Xu, "Torque Ripples and Estimation Performance of High Frequency Signal Injection based Sensorless PMSM Drive Strategies", IEEE Energy Conversion Congress and Exposition, ECCE'10, September 2010, pp. 1699-1706.
[55] Z. Anping, and W. Jian, "Observation Method for PMSM Rotor Position Based on High Frequency Signal Injection", in Conf. Rec., IEEE-ICECE, June 2010, pp. 3933-3936.
[56] D. Basic, F. Malrait, and P. Rouchon, "Initial Rotor Position Detection in PMSM based on Low Frequency Harmonic Current Injection", in IEEE Conf. Rec., 14th International Power Electronics and Motion Control Conference EPE-PEMC, September 2010, pp. 1-7.
[57] W. Staffler, and M. Schrödl, "Extended mechanical observer structure with load torque estimation for sensorless dynamic control of permanent magnet synchronous machines", in IEEE Conf. Rec., 14th International Power Electronics and Motion Control Conference EPE-PEMC, September 2010, pp. 18-22.
[58] F. De Belie, P. Sergeant, and J. A. Melkebeek, "A Sensorless Drive by Applying Test Pulses Without Affecting the Average-Current Samples", IEEE Transactions on Power Electronics, Vol. 25, No. 4, April 2010, pp. 875-888.
[59] H. Chaoui, W. Gueaieb, and M. C.E. Yagoub, "Neural Network Based Speed Observer for Interior Permanent Magnet Synchronous Motor Drives", in Conf. Rec., IEEE-EPEC, October 2009, pp. 1-6.
[60] J. L. F. Daya, V. Subbiah, "Robust Control of Sensorless Permanent Magnet Synchronous Motor Drive using Fuzzy Logic", in Conf. Rec., IEEE-ICACC, June 2010, pp. 14-18.
[61] H. Chaoui, and P. Sicard, "Sensorless Neural Network Speed Control of Permanent Magnet Synchronous Machines with Nonlinear Stribeck Friction", IEEE/ASME International Conference on Advanced Intelligent Mechatronics (AIM), July 2010, pp. 926-931.
[62] A. Accetta, M. Cirrincione, and M. Pucci, "Sensorless Control of PMSM by a Linear Neural Network: TLS EXIN Neuron", Proc. of the 36th Annual Conference of the IEEE-IECON, November 2010, pp. 974-978.
[63] C. B. Butt, M. A. Hoque, and M. A. Rahman, "Simplified Fuzzy-Logic-Based MTPA Speed Control of IPMSM Drive", IEEE Transactions on Industry Applications, Vol. 40, No. 6, November/December 2004, pp. 1529-1535.
[64] K. K. Halder, N. K. Roy, and B. C. Ghosh, "A High Performance Position Sensorless Surface Permanent Magnet Synchronous Motor Drive Based on Flux Angle", in Conf. Rec., IEEE-ICECE, December 2010, pp. 78-81.

[65] M. Hinkkanen, T. Tuovinen, L. Harnefors, and J. Luomi, "Analysis and Design of a Position Observer with Stator-Resistance Adaptation for PMSM Drives", in Conf. Rec., IEEE-ICEM, September 2010, pp. 1-6.
[66] S. Koonlaboon, and S. Sangwongwanich, "Sensorless Control of Interior Permanent Magnet Synchronous Motors Based on A Fictitious Permanent Magnet Flux Model", in Conf. Rec., IEEE-IAS'05, Vol. 1, October 2005, pp. 311-318.
[67] Y. Inoue, Y. Kawaguchi, S. Morimoto, and M. Sanada, "Performance Improvement of Sensorless IPMSM Drives in a Low-Speed Region Using Online Parameter Identification", IEEE Transactions on Industry Applications, Vol. 47, No. 2, March/April 2011, pp. 798-804.
[68] M. Hinkkanen, T. Tuovinen, L. Harnefors, and J. Luomi, "A Reduced-Order Position Observer With Stator-Resistance Adaptation for PMSM Drives", in Proc. of the IEEE-ISIE Conf., July 2010, pp. 3071-3076.
[69] Magnus Jansson, Lennart Harnefors, Oskar Wallmark, and Mats Leksell, "Synchronization at Startup and Stable Rotation Reversal of Sensorless Nonsalient PMSM Drives", IEEE Transactions on Industrial Electronics, Vol. 53, No. 2, April 2006, pp. 379-387.